

Parameter Estimation for HOSVD-based Approximation of Temporally Coherent Mesh Sequences

Michał Romaszewski and Przemysław Głomb

Institute of Theoretical and Applied Informatics, Polish Academy of Sciences, Bałtycka 5, 44-100, Gliwice, Poland

Keywords: 3D Animation, Compression, TCMS, HOSVD, Decomposition, Approximation.

Abstract: This paper is focused on the problem of parameter selection for approximation of animated 3D meshes (Temporally Coherent Mesh Sequences, TCMS) using Higher Order Singular Value Decomposition (HOSVD). The main application of this approximation is data compression. Traditionally, the approximation was done using matrix decomposition, but recently proposed tensor methods (e.g. HOSVD) promise to be more effective. However, the parameter selection for tensor-based methods is more complex and difficult than for matrix decomposition. We focus on the key parameter, the value of N -rank, which has major impact on data reduction rate and approximation error. We present the effect of N -rank choice on approximation performance in the form of rate-distortion curve. We show how to quickly create this curve by estimating the reconstruction error resulting from the N -rank approximation of TCMS data. We also inspect the reliability of created estimator. Application of proposed method improves performance of practical application of HOSVD for TCMS approximation.

1 INTRODUCTION

Three-dimensional meshes are one of the most common representations of a virtual surface with applications in computer simulations, entertainment, medical imaging and digital heritage documentation. Complexity of processing, visualization and storage of modelled objects resulted in the rapid development of methods for mesh compression, as summarised in (Maglo et al., 2015).

Particularly interesting group of methods is related to compression of temporally coherent mesh sequences (TCMS), also called dynamic animations or animated meshes, well defined in (Arcila et al., 2013). TCMS is a sequence of meshes ordered in time, with a constant number of vertices, connectivity and topology. One particularly successful approach to TCMS compression employs Principal Component Analysis (PCA). The general idea was presented in (Alexa and Muller, 2000). The animation was converted to a matrix by stacking meshes frame-by-frame. Authors represented each frame of the animation as a linear combination of principal components, obtained through decomposition of the animation matrix. Such representation allows to transmit only a limited number of first principal components and efficiently reconstruct the original sequence with limited distortion. Further

works refined this idea, e.g. the COBRA algorithm described in (Váša and Skala, 2009) reaches compression ratio between 0.5 and 5 bit per frame per vertex (bpfv) for a KG error (a measure commonly used to compare TCMS compression algorithms and described in (Karni and Gotsman, 2004)) of 0.05%.

As an alternative to matrix approximation, TCMS data can be expressed in the form of a mode-3 tensor \mathcal{T} and tensor decomposition may be employed. One particularly suitable method is the Higher Order Singular Value Decomposition (HOSVD), described in detail in (Kolda and Bader, 2009). Its recent application to data compression was presented e.g. in (Ballester-Ripoll and Pajarola, 2015).

HOSVD transforms the mode-3 TCMS tensor \mathcal{T} into the Tucker operator (TO). The TO consist of the core tensor \mathcal{C} and three orthogonal factor matrices. The key property of this representation is the approximation. The energy of the core tensor is concentrated in the frontal-upper-left corner so large magnitudes correspond to its low indices. The TO can be truncated by zeroing the low-index elements, forming a truncated Tucker operator (TTO). Original data can be reconstructed from the TTO with the reconstruction error expressed in the form of tensor Frobenius norm as $\|\mathcal{T} - \mathcal{T}'\|$.

When applied to TCMS data, HOSVD may al-

low to reach higher data reduction ratio with lower distortion than PCA, as presented in (Romaszewski et al., 2013), where authors compare HOSVD and PCA applied to lossy reconstruction of TCMS sequences. They present the performance of these methods in terms of data size and reconstruction error for a set of well-known, representative sequences.

The main challenge, however, when applying HOSVD for TCMS compression lies in finding the N -rank value to minimize the TTO size with an acceptable reconstruction error. Usually (e.g. in (Romaszewski et al., 2013)) this is done by searching through the parameter space. Since the reconstruction of \mathcal{T} from TTO is computationally expensive, the questions arise: how to estimate the reconstruction error associated with the specific N -rank, how to find its optimal value and how reliable is such estimation for TCMS data?

This paper concentrates on the problem of N -rank estimation for approximating TCMS data with HOSVD. The distortion resulting from approximation is expressed in the form of KG error, commonly used to compare TCMS compression methods. We show how to use the estimator to graphically represent the effect of HOSVD reconstruction in the form of a rate-distortion curve. We also discuss the estimation reliability using a set of well-known TCMS samples.

The article is organised as follows. The introduction and related work are presented in Section 1. Definitions and methodology are presented in Section 2. Results are presented in Section 3, while conclusions can be found in Section 4.

2 METHODOLOGY

Our goal is to estimate the error associated with the N -rank approximation of the TCMS tensor \mathcal{T} using the HOSVD algorithm. We use this estimation to form the rate-distortion curve based on N -rank TTO truncation.

2.1 Input Data

Our input data is the temporally coherent mesh sequence (TCMS), described in detail in (Arcila et al., 2013). Such sequence consists of meshes with constant connectivity and varying positions of vertices in time. We consider only the vertex position data, since it has the most significant impact on animation volume. Animation vertices can be represented as a sequence of F matrices $\mathbf{M}_k \in \mathbb{R}^{K \times J}$. The rows of \mathbf{M}_k are positions of mesh vertices $v_i \in \mathbb{R}^J, 0 \leq i < K$. These matrices can form a tensor $\mathcal{T} = t_{i,j,k} \in \mathbb{R}^{K,J,F}$

by stacking \mathbf{M}_k as frontal slices $\mathcal{T}_{:,k}$, using the notation from (Kolda and Bader, 2009). In our experiments vertex features are the standard euclidean coordinates only, therefore $J = 3$.

2.2 Higher Order Singular Value Decomposition

Higher Order Singular Value Decomposition is a generalisation of SVD from matrices to tensors. Based on description provided in (Romaszewski et al., 2013) and following the conventions presented in (Kolda and Bader, 2009), HOSVD can be explained in the following way:

A tensor

$$\mathcal{T} = \{t_{i_1, i_2, \dots, i_n}\}_{i_1, i_2, \dots, i_n=0}^{I_1-1, I_2-1, \dots, I_N-1} \in \mathbb{R}^{I_1, I_2, \dots, I_N} \quad (1)$$

has N modes. Each of the indices corresponds to one of the modes *i.e.* i_l to mode l .

By *multiplication* of tensor \mathcal{T} by matrix $\mathbf{U} = \{u_{ij}\}_{i,j=0}^{I_l-1, D} \in \mathbb{R}^{I_l, D}$ in mode l we define tensor $\mathcal{T}' \in \mathbb{R}^{I_1, \dots, I_{l-1}, D, I_{l+1}, \dots, I_N}$, such that:

$$\mathcal{T}' = (\mathcal{T} \times_l \mathbf{U})_{i_1, \dots, i_{l-1}, d, i_{l+1}, \dots, i_N} = \sum_{i_l=0}^{I_l-1} t_{i_1, i_2, \dots, i_l, \dots, i_N} u_{i_l, d}. \quad (2)$$

By *unfolding* tensor \mathcal{T} in mode l we define matrix $\mathbf{T}_{(l)}$ such that

$$(\mathbf{T}_{(l)})_{i,j} = t_{i_1, \dots, i_{l-1}, j, i_{l+1}, \dots, i_N}, \quad (3)$$

where $i = 1 + \sum_{k=1, k \neq l}^N (i_k - 1)J_k$ and $J_k = \prod_{m=1, m \neq l}^{k-1} I_m$.

Given tensor \mathcal{T} , defined as in Eq. (1), a new *sub-tensor* $\mathcal{T}_{i_n=\alpha}$ can be created according to the equation with the following elements:

$$\mathcal{T}_{i_n=\alpha} = \{t_{i_1, i_2, \dots, i_{l-1}, i_{l+1}, \dots, i_n}\}_{i_1=0, i_2=0, \dots, i_l=\alpha, \dots, i_n=0}^{I_1-1, I_2-1, \dots, \alpha, \dots, I_N-1} \quad (4)$$

where

$$\mathcal{T}_{i_n=\alpha} \in \mathbb{R}^{I_1, I_2, \dots, 1, \dots, I_N}. \quad (5)$$

The *scalar product* $\langle \mathcal{A}, \mathcal{B} \rangle$ of tensors $\mathcal{A}, \mathcal{B} \in \mathbb{R}^{I_1, I_2, \dots, I_N}$ is defined as

$$\langle \mathcal{A}, \mathcal{B} \rangle = \sum_{i_1=0}^{I_1-1} \sum_{i_2=0}^{I_2-1} \dots \sum_{i_N=0}^{I_N-1} b_{i_1, i_2, \dots, i_N} a_{i_1, i_2, \dots, i_N}. \quad (6)$$

We say that if scalar product of tensors equals zero, then they are orthogonal.

The *Frobenius norm* of tensor \mathcal{T} is given by $\|\mathcal{T}\| = \sqrt{\langle \mathcal{T}, \mathcal{T} \rangle}$.

Given tensor \mathcal{T} , in order to find its HOSVD, in the form of the so called Tucker operator $[[\mathcal{C}; \mathbf{U}^{(1)}, \dots, \mathbf{U}^{(N)}]]$, such that $\mathcal{C} \in \mathbb{R}^{I_1, \dots, I_N}$ and $\mathbf{U}^{(k)} \in \mathbb{R}^{I_k, I_k}$ are orthogonal matrices, Algorithm 1 can be used.

Tensor \mathcal{C} is called the core tensor and has the following useful properties. Reconstruction: $\mathcal{T} = \mathcal{C} \times_1 \mathbf{U}^{(1)} \times_2 \mathbf{U}^{(2)} \times_3 \dots \times_N \mathbf{U}^{(N)}$, where $\mathbf{U}^{(i)}$ are orthogonal matrices. Orthogonality: $\langle \mathbf{C}_{i=\alpha}, \mathbf{C}_{i=\beta} \rangle = 0$ for all possible values of l , α and β , such that $\alpha \neq \beta$. Order of sub-tensor norms: $\|\mathbf{C}_{i_n=1}\| \leq \|\mathbf{C}_{i_n=2}\| \leq \dots \leq \|\mathbf{C}_{i_n=l_n}\|$ for all n .

Input: Data Tensor \mathcal{T}
Output: Tucker operator $\llbracket \mathcal{C}; \mathbf{U}^{(1)}, \dots, \mathbf{U}^{(N)} \rrbracket$
for $k \in \{1, \dots, N\}$ **do**
 $\mathbf{U}^{(k)} =$
 left singular vectors of $\mathbf{T}_{(k)}$ in unfolding k ;
end
 $\mathcal{C} = \mathcal{T} \times_1 \mathbf{U}^{(1)\top} \dots \times_N \mathbf{U}^{(N)\top}$;
return $\llbracket \mathcal{C}; \mathbf{U}^{(1)}, \dots, \mathbf{U}^{(N)} \rrbracket$;

Algorithm 1: HOSVD algorithm used to find the Tucker operator from the tensor \mathcal{T} .

Therefore, informally, one can say that larger magnitudes of a core tensor are denoted by low values of indices. To explain the HOSVD approximation we will define the tensor

$$\tilde{\mathcal{T}} = \tilde{\mathcal{C}} \times_1 \tilde{\mathbf{U}}^{(1)} \times_2 \tilde{\mathbf{U}}^{(2)} \times_3 \dots \times_N \tilde{\mathbf{U}}^{(N)}, \quad (7)$$

where

$$\tilde{\mathcal{C}} = \{c_{i_1, i_2, \dots, i_n}\}_{i_1=0, \dots, i_n=0}^{R_1-1, R_2-1, \dots, R_N-1} \in \mathbb{R}^{R_1, R_2, \dots, R_N} \quad (8)$$

is a truncated tensor in such a way that in each mode l indices span from 0 to $R_l - 1 \leq I_l - 1$ and $\tilde{\mathbf{U}}^{(l)} \in \mathbb{R}^{R_l, I_l}$ matrices whose columns are orthonormal and rows form orthonormal basis in respective vector spaces. Given $(R_l)_{l=1}^N$ we say that $\tilde{\mathcal{T}}$ approximates \mathcal{T} in the sense of their euclidean distance $\|\tilde{\mathcal{T}} - \mathcal{T}\|$.

2.3 Estimation of Reconstruction Error

One way of finding the optimal (given the error threshold) N -rank value for the data tensor \mathcal{T} , is to perform multiple reconstructions of \mathcal{T} from TTT. Unfortunately, such search is time consuming. It could be, however, avoided with a reliable estimator of the N -rank reconstruction error. Our task is therefore to define the reconstruction error metric, to find an estimator, and to assess its reliability.

2.3.1 The Metric for Reconstruction Error

We argue that the most useful error metrics for the TCMS reconstruction estimator would be the distortion measure used to compare TCMS compression algorithms, namely the KG error. The KG error was

defined in (Karni and Gotsman, 2004) to express the distortion of TCMS compression based on PCA. Its benefit is that it allows to compare the distortion introduced by HOSVD-based approximation with the final results of state-of-art TCMS compression algorithms. It should be noted, however, that KG error does not correlate well with perceptual distortion of animations and its shortcomings were noted e.g. in (Váša and Skala, 2009). Since the KG error was originally defined using matrix operations, we will express it using the tensor notation in the following way:

Given tensor $\mathcal{T} = t_{i,j,k} \in \mathbb{R}^{K,J,F}$ we define the average trajectory tensor $E(\mathcal{T}) = e_{i,j,k} \in \mathbb{R}^{K,J,F}$ in which each mode-3 (tube) fiber is substituted by an average mode-3 fiber of \mathcal{T} , so $e_{ijk} = \text{avg}_{1 < k' \leq F} (t_{ijk'})$.

This allows us to express the KG error as

$$e_{kg}(\mathcal{T}, \tilde{\mathcal{T}}) = 100 \frac{\|\mathcal{T} - \tilde{\mathcal{T}}\|}{\|\mathcal{T} - E(\mathcal{T})\|}. \quad (9)$$

2.3.2 The Estimation of the N -rank Reconstruction Error

An estimator for the upper bound of HOSVD reconstruction error may be found in (De Lathauwer et al., 2000). It is expressed in the form of the following property.

Let the HOSVD of \mathcal{T} be given and let ranks of \mathcal{T} in unfolding $\mathbf{T}_{(n)}$ be equal to R_n ($1 \leq n \leq N$). Define a tensor $\tilde{\mathcal{T}}$ by discarding the smallest singular values $\sigma_{I'_n+1}^{(n)}, \sigma_{I'_n+2}^{(n)}, \dots, \sigma_{R_n}^{(n)}$ for given values of I'_n ($1 \leq n \leq N$) in unfolding $\mathbf{T}_{(n)}$, i.e., set the rest of them to zero. Then we have

$$\|\mathcal{T} - \tilde{\mathcal{T}}\|^2 \leq E(I'_1 + 1, \dots, I'_N + 1). \quad (10)$$

where

$$E(I'_1, \dots, I'_N) = \sum_{i_1=I'_1+1}^{R_1} \sigma_{i_1}^{(1)2} + \dots + \sum_{i_N=I'_N+1}^{R_N} \sigma_{i_N}^{(N)2}. \quad (11)$$

The nature of this estimation allows us to conclude two useful properties of HOSVD reconstruction. Firstly, the upper bound of reconstruction error is no higher than the sum of errors resulting from each $\mathbf{T}_{(n)}$ unfolding truncation. This means that we can treat the truncation of each mode separately for the purpose of reconstruction parameter selection. Secondly, the error is proportional to the sum of squared singular values discarded from $\mathbf{T}_{(n)}$ decomposition. Therefore the value of error will rapidly decrease for small number of first components.

Based on equations (9) and (10), we can estimate the upper bound of the KG error for the N -rank reconstruction of \mathcal{T} as:

$$e_{kg}^{(est)}(\mathcal{T}, \tilde{\mathcal{T}}) = 100 \frac{\sqrt{E(I'_1 + 1, \dots, I'_N + 1)}}{\|\mathcal{T} - E(\mathcal{T})\|}. \quad (12)$$

where $e_{kg}(\mathcal{T}, \tilde{\mathcal{T}}) \leq e_{kg}^{(\text{est})}(\mathcal{T}, \tilde{\mathcal{T}})$.

If we further assume that the estimation of error with Eq. (10) is saturated for TCMS data, i.e. it's close to the actual reconstruction error, we can use this estimation to find the optimal N -rank.

In order to test this estimation reliability we will define the relative estimator error as

$$\psi(\mathcal{T}, \tilde{\mathcal{T}}) = \frac{|e_{kg}(\mathcal{T}, \tilde{\mathcal{T}}) - e_{kg}^{(\text{est})}(\mathcal{T}, \tilde{\mathcal{T}})|}{e_{kg}(\mathcal{T}, \tilde{\mathcal{T}})}. \quad (13)$$

2.3.3 The Choice of Reconstruction Parameters

Input: The rate array \mathbf{R} and the corresponding distortion array \mathbf{D} .

Output: Sequence of distortions \mathbf{d}_{rd} and corresponding reduction rates \mathbf{r}_{rd}

```

 $\mathbf{d} = \text{vec}(\mathbf{D});$ 
 $\mathbf{r} = \text{vec}(\mathbf{R});$ 
 $\mathbf{i} = \text{argsort } \mathbf{d}$  in ascending order;
sort  $\mathbf{d}, \mathbf{r}$  with  $\mathbf{i}$ ;
 $\mathbf{d}_{rd} = [];$ 
 $\mathbf{r}_{rd} = [];$ 
for  $i \in \{1, \dots, \text{length}(\mathbf{d})\}$  do
    if is empty  $\mathbf{r}_{rd}$  or  $\mathbf{r}_{rd}[i] < \mathbf{r}_{rd}[i-1]$  then
        append  $\mathbf{d}[i]$  to  $\mathbf{d}_{rd}$ ;
        append  $\mathbf{r}[i]$  to  $\mathbf{r}_{rd}$ ;
    end
end
return  $(\mathbf{d}_{rd}, \mathbf{r}_{rd})$ 
    
```

Algorithm 2: The algorithm to create the rate-distortion curve by computing the sequence of reconstruction errors \mathbf{d}_{rd} and corresponding reduction rates \mathbf{r}_{rd} .

The choice of the N -rank value that minimizes the TTO size while also minimizing the reconstruction error is not obvious. Desired values depend on the specific application of the algorithm. Their mutual relation may be presented graphically in the form of the rate-distortion curve in the following way:

The TCMS tensor $\mathcal{T} = t_{i,j,k} \in \mathbb{R}^{K,J,F}$ can be approximated by the N -rank tensor $\tilde{\mathcal{T}}$ with the error $e_{kg}(\mathcal{T}, \tilde{\mathcal{T}})$. The $e_{kg}(\mathcal{T}, \tilde{\mathcal{T}})$ value can be estimated from the Eq. (12). The N -rank is a reconstruction parameter denoted $\mathbf{rank}_N(\mathcal{T}) = (R_1, R_2, R_3)$. The number of possible N -ranks of \mathcal{T} is $R_1 \times R_2 \times R_3$. However, the second mode of the TCMS tensor is short since $J = 3$ and the mode-2 truncation introduces huge distortion into the approximation. Therefore, we only consider the truncation of mode-1 and mode-3 components. We denote the N -rank reconstructed tensor $\tilde{\mathcal{T}}_{ik}$ such that $\mathbf{rank}_N(\tilde{\mathcal{T}}_{ik}) = (i, 3, k)$.

The number of floats required to store the $\tilde{\mathcal{T}}_{ik}$ equals $S(\tilde{\mathcal{T}}_{ik}) = i \times K + 9 + k \times F + i \times 3 \times k$. The

data reduction rate resulting from using $\tilde{\mathcal{T}}_{ik}$ can be expressed as

$$\Theta(\tilde{\mathcal{T}}_{ik}) = \frac{S(\tilde{\mathcal{T}}_{ik})}{K \times J \times F}. \quad (14)$$

We will define a rate array as $\mathbf{R} = \{a_{ik}\}$ where $a_{ik} = \Theta(\tilde{\mathcal{T}}_{ik})$ and a corresponding distortion array $\mathbf{D} = \{b_{ik}\}$ such that $b_{ik} = e_{kg}(\mathcal{T}, \tilde{\mathcal{T}}_{ij})$. This allows us to define a sequence of all pairs $RD = ([a_m, b_m])$ where $a_m \in \mathbf{R}$, $b_m \in \mathbf{D}$, and the $[a_m, b_m]$ pairs are ordered such that $\forall_m a_{m-1} < a_m$ and $\forall_m b_{m-1} > b_m$. To obtain this sequence we use the simple algorithm presented as Alg. (2). The graphical representation of this sequence is the rate-distortion curve of \mathcal{T} .

2.4 Principal Component Analysis

As a reference for approximation of TCMS data with HOSVD, we use the Principal Component Analysis described e.g. in (Jolliffe, 2005). We follow the methodology described in (Romaszewski et al., 2013). In order to apply the PCA, tensor $\mathcal{T} = t_{i,j,k} \in \mathbb{R}^{K,J,F}$ is unfolded according to Eq. (3). We consider a mode-3 (frame) unfolding which forms the matrix $\mathbf{X} \in \mathbb{R}^{F,J \times K}$.

3 EXPERIMENT RESULTS

The goal of our experiments is to assess the reliability of error estimation for N -rank HOSVD reconstruction of TCMS.

3.1 Implementation Setup

We apply the HOSVD algorithm presented as Alg. (1) to samples of TCMS data. Then, for all possible N -rank values we reconstruct $\tilde{\mathcal{T}}_{ik}$ and compute $e_{kg}(\mathcal{T}, \tilde{\mathcal{T}}_{ik})$ using the Eq. (9). We also estimate N -rank reconstruction error using the Eq. (12). We compute the estimator error as $\psi(\mathcal{T}, \tilde{\mathcal{T}}_{ik})$ using the Eq. (13). We present the relation between the reconstruction and estimation errors in the form of a rate-distortion curve. Results are presented using four standard TCMS sequences. The *chicken* is an artificial animation of a running cartoon character, published by Jed Lengyel¹. *Crane*, *samba* and *march* are motion capture sequences published by Daniel Vlasic².

¹<http://jedwork.com/jed>

²http://people.csail.mit.edu/draniel/mesh_animation

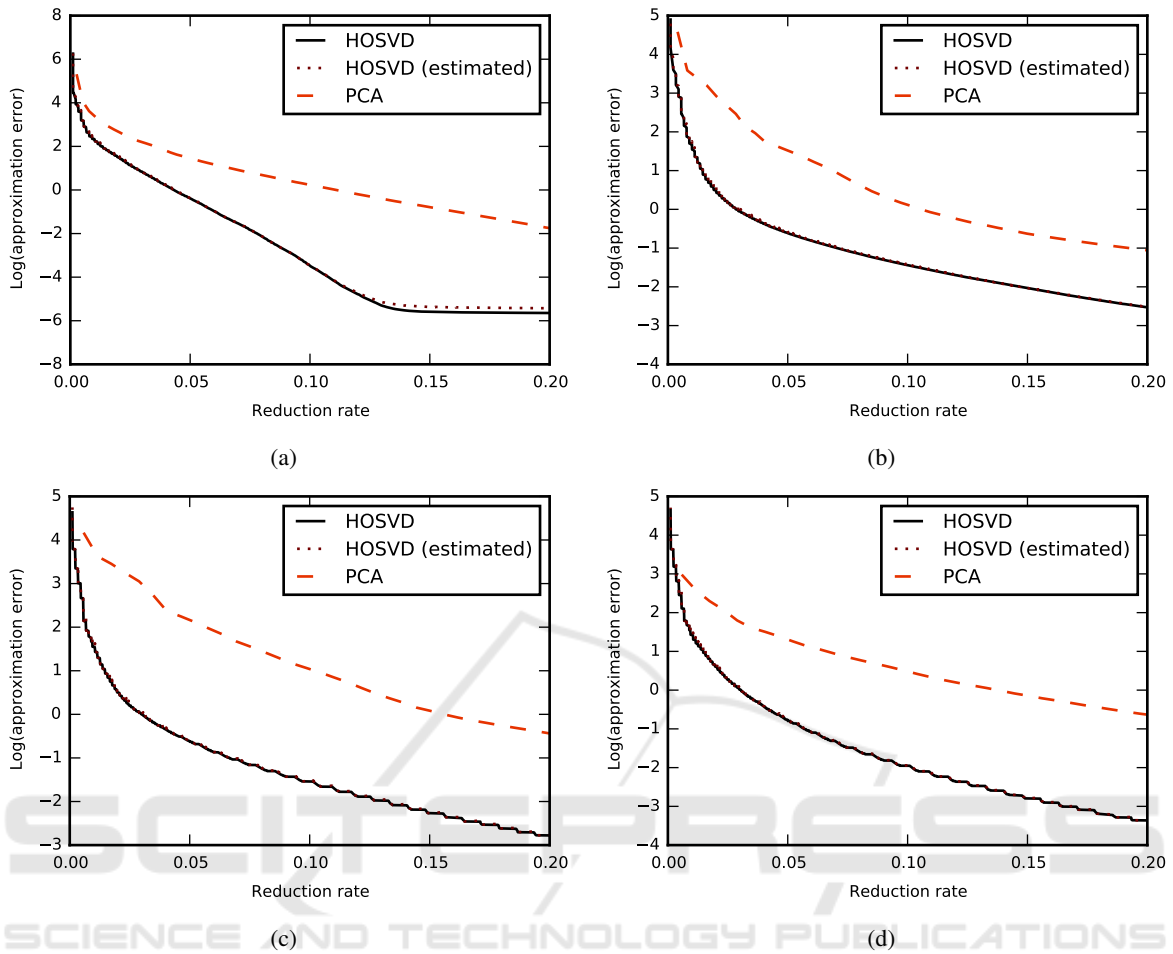


Figure 1: Rate-distortion curves for animations: *chicken* (a), *march* (b), *crane* (c), *samba* (d). The horizontal axis represents the reduction rate $\Theta(\tilde{\mathcal{T}}_{ik})$ and the vertical axis is the logarithm of reconstruction error $e_{kg}(\mathcal{T}, \tilde{\mathcal{T}})$. Plots present actual and estimated error values for HOSVD. Error values for PCA are provided for reference. The difference between the estimated and actual values of approximation error for HOSVD are very small.

3.2 Results

The reconstruction error introduced by HOSVD approximation of TCMS data is presented in Fig. 3. Each pixel in panels (a), (c) and (e) represents the N -rank reconstruction while axes show the number of mode-1 and mode-3 components. The error is monotonic and it drops sharply from the highest value in the lower-left corner (reconstruction from only one component in both modes) to the low error value in the upper-right corner. The perceptual distortion of reconstructed animation becomes very small for ~ 50 mode-1 and mode-3 components which corresponds to values lying above and on the right from the isoline zero.

Panels (b), (d) and (f) in Fig. 3 represent the corresponding values of the estimation error $\psi(\mathcal{T}, \tilde{\mathcal{T}}_{ik})$. We can imminently see that $\psi(\mathcal{T}, \tilde{\mathcal{T}}_{ik})$ values are small.

That means that the error estimation obtained using Eq. (12) is close to its actual value. However, it is apparent that the estimation is more accurate for large error values in the upper-left and lower-right corners, separated with the isoline (-8) . At the same time an obvious strategy for optimal N -rank choice are the values close to the diagonal line connecting the lower-left and upper-right corners of the array. These parameters results in low reconstruction error but are also less accurately estimated. Nevertheless, for parameters representing the perceptually acceptable TCMS approximation, the estimation is accurate enough that there is no difference in the parameter choice based on estimated or accurate error values.

The rate-distortion curves for actual and estimated values of HOSVD approximation error are presented in Fig. 1. PCA approximation error is provided for reference. The perceptual distortion of the animation

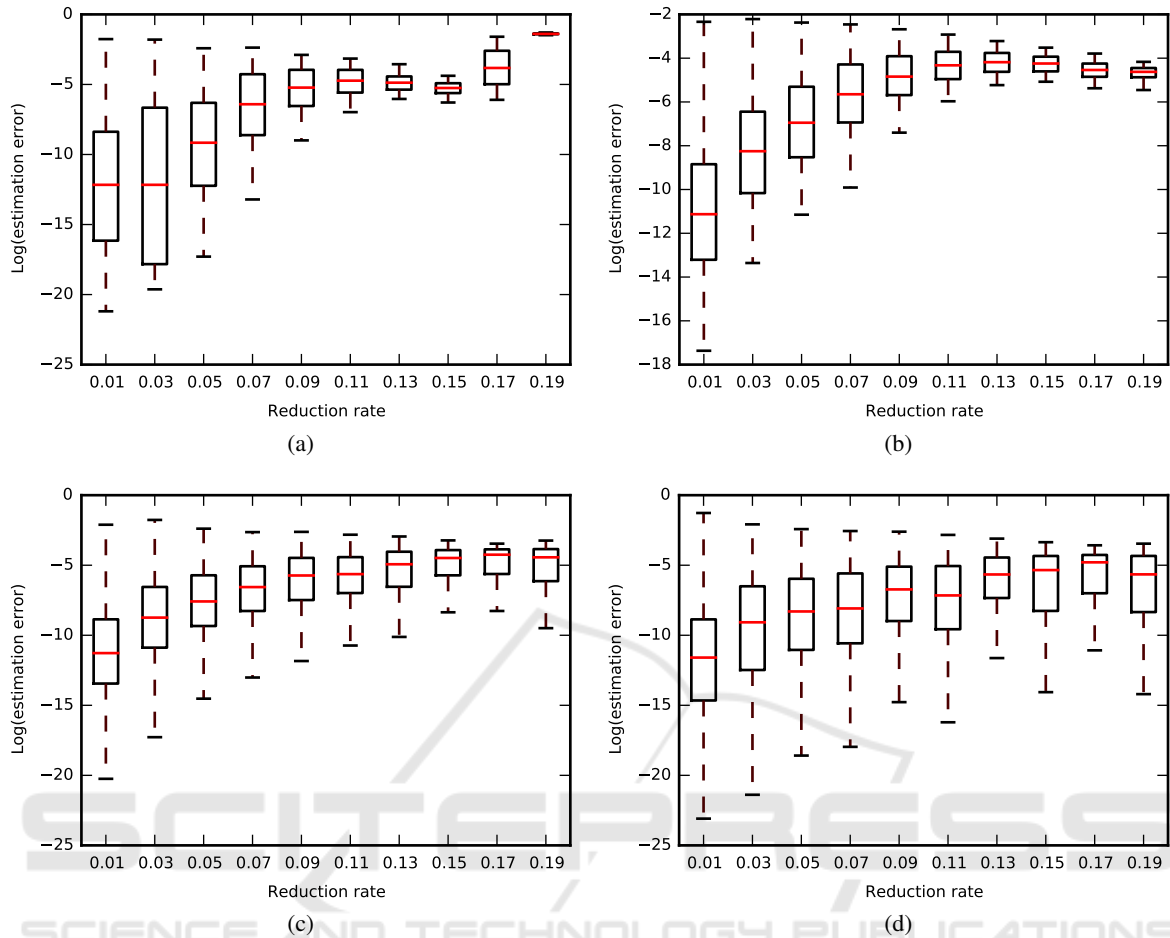


Figure 2: Estimation error for animations: *chicken* (a), *march* (b), *crane* (c), *samba* (d). The horizontal axis represents the reduction rate $\Theta(\tilde{\mathcal{T}}_{ik})$ and the vertical axis is the logarithm of estimation error $\psi(\mathcal{T}, \tilde{\mathcal{T}}_{ik})$. Each error bar represents the median, lower and upper quartile as well as error range in one of ten non-overlapping windows of equal length. Values on the horizontal axis are in the middle of a corresponding window.

becomes acceptable for reduction rate $\sim 5\%$ original data size, and almost indistinguishable when the reduction rate is $\sim 10\%$ of the original size.

Fig. 2 is the visualization of estimation error for our animations. Each error bar represents the median, lower and upper quartile and error range in the ten non-overlapping horizontal windows. As we can see the estimation is more precise for high reduction rate, but with significant variance. This is more visible for artificial *chicken* sequence than for motion-capture animations. This effect results mostly from the improper estimation for very low N -rank values located in the lower-left corner of the parameter array. On the other hand, for lower reduction rate the estimator is less precise but with a low variance.

4 CONCLUSIONS

We have shown how to estimate the N -rank HOSVD reconstruction error for TCMS data. We argue that for representative sequences the estimator is saturated. That means that the estimated distortion is very close to its actual value and can aid in selection of approximation parameters. Expressing the distortion resulting from approximation of \mathcal{T} in the form of KG error is useful during the creation of HOSVD-based TCMS compression algorithms.

ACKNOWLEDGEMENTS

This work has been partially supported by the project ‘Representation of dynamic 3D scenes

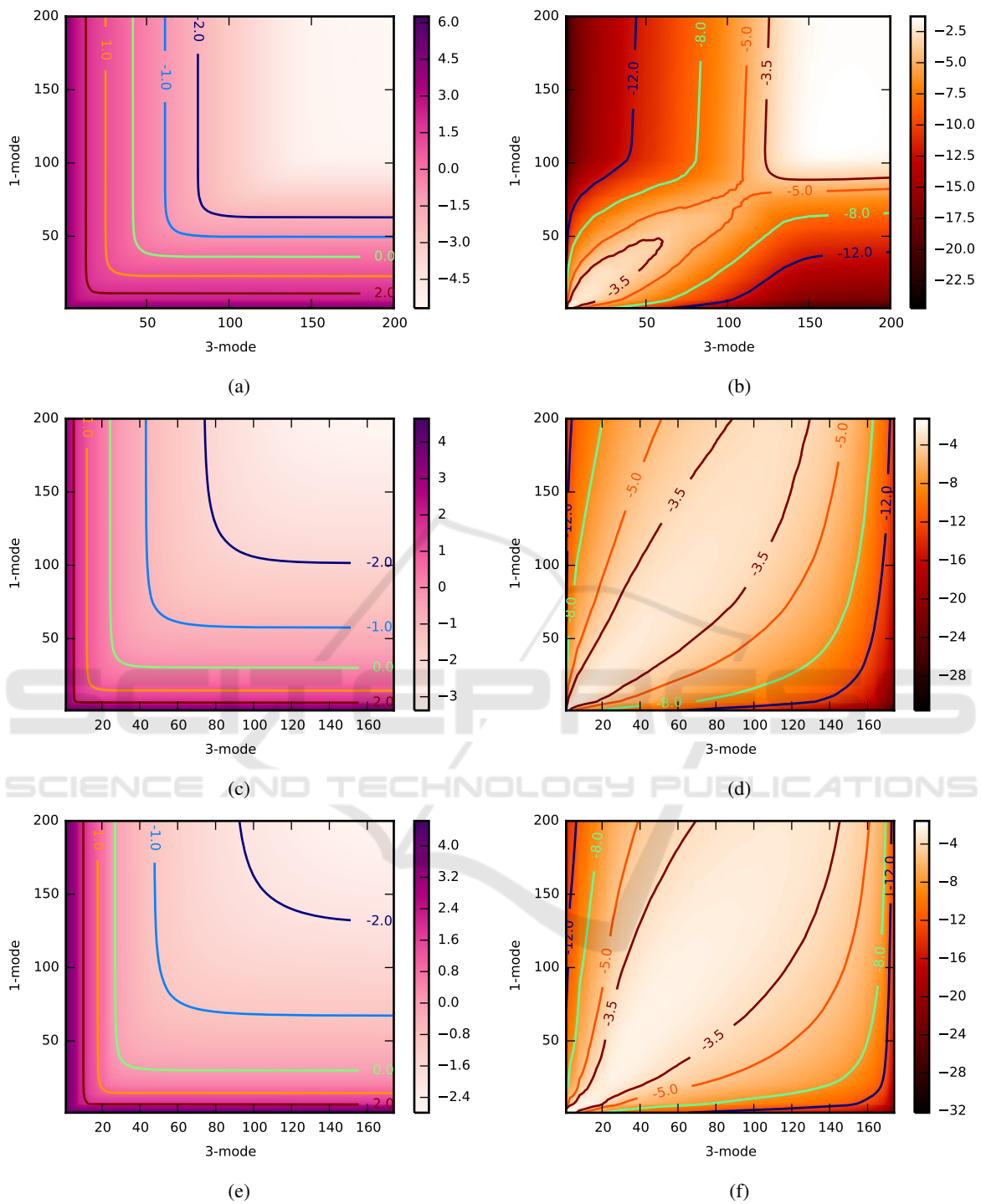


Figure 3: Reconstruction and estimation errors for three animations: *chicken* (the upper row), *crane* (the middle row), *samba* (the lower row). Pixels in arrays (a),(c) and (e) represent the logarithm of $e_{kg}(\mathcal{T}, \hat{\mathcal{T}}_{ik})$ as a function of the number of mode-1 and mode-3 components used for reconstruction. Arrays (b),(d) and (f) present the corresponding estimation errors $\psi(\mathcal{T}, \hat{\mathcal{T}}_{ik})$ defined by Eq. (13).

using the Atomic Shapes Network model' financed by National Science Centre, decision DEC-2011/03/D/ST6/03753. We would like to thank our

reviewers for their insightful comments. We would also like to thank P. Gawron for fruitful discussions.

REFERENCES

- Alexa, M. and Muller, W. (2000). Representing animations by principal components. In *Computer Graphics Forum*, volume 19, pages 411–418. Citeseer.
- Arcila, R., Cagniart, C., Hétry, F., Boyer, E., and Dupont, F. (2013). Segmentation of temporal mesh sequences into rigidly moving components. *Graphical Models*, 75(1):10–22.
- Ballester-Ripoll, R. and Pajarola, R. (2015). Lossy volume compression using tucker truncation and thresholding. *The Visual Computer*, pages 1–14.
- De Lathauwer, L., De Moor, B., and Vandewalle, J. (2000). A multilinear singular value decomposition. *SIAM journal on Matrix Analysis and Applications*, 21(4):1253–1278.
- Jolliffe, I. (2005). *Principal component analysis*. Wiley Online Library.
- Karni, Z. and Gotsman, C. (2004). Compression of soft-body animation sequences. *Computers & Graphics*, 28(1):25–34.
- Kolda, T. G. and Bader, B. W. (2009). Tensor Decompositions and Applications. *SIAM Review*, 51(3):455–500.
- Maglo, A., Lavoué, G., Dupont, F., and Hudelot, C. (2015). 3d mesh compression: Survey, comparisons, and emerging trends. *ACM Computing Surveys (CSUR)*, 47(3):44.
- Romaszewski, M., Gawron, P., and Opozda, S. (2013). Dimensionality reduction of dynamic mesh animations using ho-svd. *Journal of Artificial Intelligence and Soft Computing Research*, 3(4):277–289.
- Váša, L. and Skala, V. (2009). Cobra: Compression of the basis for pca represented animations. In *Computer Graphics Forum*, volume 28, pages 1529–1540. Wiley Online Library.